

## Effect of Material Characteristics on Wrinkling During Dome Forming of a Beverage Can using LS-DYNA<sup>®</sup>

R.E. Dick and J.W. Yoon

*Alcoa Technical Center*

*100 Technical Dr., Alcoa Center, PA 15069-0001, USA*

### Abstract

*Wrinkling of thin sheet metal products such as beverage cans continues to be experienced by can manufacturers and is observed with some aluminum material suppliers more than others. These wrinkles are caused by compressive instabilities during forming, and with small base diameter cans and light gauge material, the likelihood of this wrinkle formation increases. Manufacturing experience suggests that dome wrinkling is influenced by many factors such as mechanical properties of the aluminum sheet, tooling geometry, contact conditions including the effects of lubrication, and other process boundary conditions. It is also difficult to conduct an experimental analysis of compressive instabilities of these thin sheet metal products because the effects of all of the factors contributing to the instabilities are complex and small changes in these factors may produce widely varying results. Therefore, a numerical approach is recommended to separate the effect of each variable on wrinkle formation. This paper shows how strain-hardening and *r*-values influence wrinkle formation in its magnitude and frequency through dome forming of a beverage can based on a recent anisotropic yield function implemented as an LS-DYNA UMAT subroutine.*

### Background

In the United States, lightweighting of aluminum drawn and ironed (D&I) beverage cans has been a continuous process for over 35 years. Advances in can manufacturing technology and cost control efforts by aluminum suppliers, can makers, and fillers have resulted in a consistent reduction of the net metal weight and cost of the beverage can. To reduce the weight and cost of the can bodies, cans with thinner sidewalls, reduced neck diameters and smaller base diameters have been developed. Small base diameter cans and light gauge material increase the likelihood of wrinkling during can production. Manufacturing experience suggests that dome wrinkling is influenced by many factors such as mechanical properties of the aluminum sheet, tooling geometry, contact conditions including the effects of lubrication, and other process boundary conditions. The most common wrinkling control techniques employed in the industry include increased retainer pressure and proper maintenance of tooling surface conditions. Other methods can provide increased resistance to metal flow and inhibit wrinkling but may lead to increased thinning and fracture.

Two types of wrinkling analyses are performed with the finite element method: A bifurcation analysis of a structure having no imperfections and a non-bifurcation analysis, which assumes an initial imperfection or perturbation force due to load eccentricities. Because the finite element analyses of sheet metal forming processes involve strong nonlinearities in geometry, material, and contact, convergence problems are frequently observed. Non-bifurcation analyses sometimes lead to reasonable results since all real structures have inherent imperfections, such as material non-uniformity or geometric irregularities. Therefore, most wrinkling analyses have been carried out using a non-bifurcation analysis [1,2]. However, the results obtained by non-bifurcation analysis are sensitive to the amplitude of the initial imperfections, which are chosen arbitrarily. A

sophisticated bifurcation algorithm was implemented into the finite element method in order to analyze the wrinkling behavior of sheet metal during forming more rigorously [3].

In this work, non-bifurcation analyses based on an explicit method are carried out for simplification purposes. A numerical technique for calculating a wrinkle factor, or severity of wrinkling, in the dome profile using the output from an LS-DYNA finite element analysis is employed. Using this wrinkle factor, and a fully parametric input generator, effects of material characteristics including the yield stress, strain hardening, and strain hardening rate on formability are investigated. The formability is evaluated by monitoring both the wrinkling magnitude and plastic strains during the dome forming process.

### Dome Forming Model

A schematic of the dome forming process is provided in Figure 1. A photograph showing typical dome wrinkling from a commercial can plant is provided in Figure 2. Finite element models were created to investigate the effect of material properties on wrinkling during the dome forming process. All input data files for the LS-DYNA models were generated using the LS-INGRID pre-processor. The modeled tooling consists of the punch, doming die, and pressure pad (retainer). No history of the cup forming process or the redraw process is accounted for in the redrawn cup in the dome forming model. The mechanical properties for the 3104-H1E38 alloy were input in the *as-rolled* condition. The material model is an elastic-plastic von Mises material with isotropic hardening and an arbitrary stress versus strain curve. Young's modulus is 10 million psi and Poisson's ratio is 0.33. The strain hardening of the material is described using the Voce equation:

$$\sigma = A - B \cdot \exp(-C\varepsilon)$$

where  $\sigma$  is the true stress,  $\varepsilon$  is the true plastic strain, and  $A$ ,  $B$ ,  $C$  are the Voce material constants. The material input data for all cases analyzed are provided in Table 1.

A typical predicted formed shape of a beverage can dome profile showing profile wrinkling is provided in Figure 3. A radial coordinate contour plot of the wrinkled dome profile is shown in Figure 4. The plot shows the radial distance and circumferential position for each circumferential ring of nodes in the wrinkled region of the dome profile. The wrinkle factor is calculated as the percentage of the maximum normalized arc length relative to the unit length calculated from each contour based on the radial coordinate plot data. A wrinkle factor of zero indicates no wrinkling.

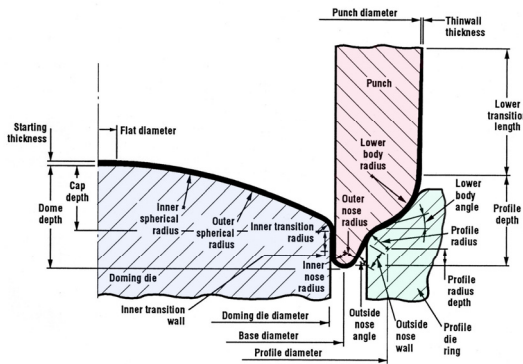


Figure 1. Schematic of the dome forming process.



Figure 2. Photograph of beverage can showing dome profile wrinkles.



Figure 3. Typical beverage can dome showing profile wrinkles.

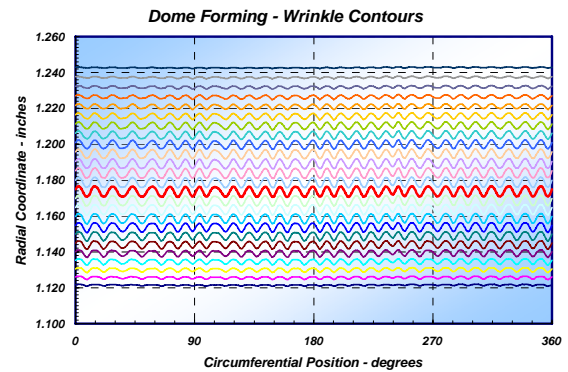


Figure 4. Radial coordinate contour plot for beverage can dome profile.

### Effect of Material Characteristics

In order to investigate the impact of material characteristics on dome wrinkling, a numerical design of experiments was generated. A 2<sup>3</sup> factorial design evaluating the three voce coefficients at two levels was used. Additionally, several single variable analysis studies were included to independently study the impact of yield stress, strain hardening (with constant yield stress and with constant tensile stress), and strain hardening rate. The response variable is the wrinkle factor. The effective plastic strains were also extracted from the FEM models. The complete experimental design is given in Table 1. The range of values chosen is considered typical of *as-rolled* properties for existing body stock alloys.

The calculated wrinkle factors and predicted maximum effective plastic strains for each of the cases are also summarized in Table 1. A plot of the voce curves and predicted wrinkle factors for the factorial design is given in Figure 5. A Yates analysis of the factorial design data (Attachment 1) shows the average effect of the A coefficient is 9.4, the average effect of the B coefficient is -3.5, and the average effect of the C coefficient is 9.1. The data suggests that a material stress-strain curve (defined using the voce equation) with a low A value, a high B value, and a low C value will minimize dome profile wrinkling. This indicates that materials with a low yield stress, low strain hardening, and a low strain hardening rate will produce a dome with minimal wrinkling.

To further clarify the results, single variable analyses were examined. The effect of yield stress is summarized in Figure 6 and shows lower wrinkle factors as the yield stress is reduced. The effect of strain hardening assuming a constant yield stress is provided in Figure 7 and shows that lower strain hardening also reduces the wrinkle factor. The effect of strain hardening assuming a constant tensile stress is shown in Figure 8 and indicates reduced wrinkling with increased hardening (lower yield stress), particularly for materials with low hardening rates. The impact of the strain hardening rate is displayed in Figure 9 and demonstrates reduced wrinkle factors with lower hardening rates.

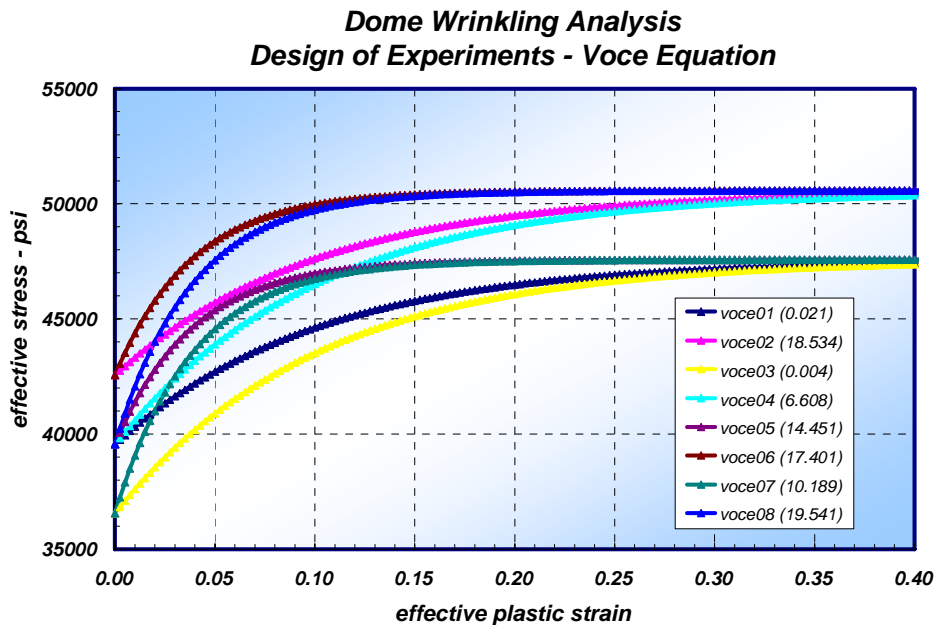


Figure 5. Voce curves and predicted wrinkle factors for 2<sup>3</sup> factorial design of experiments.

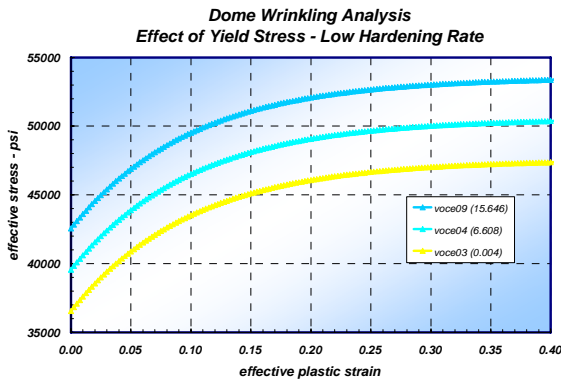


Figure 6. Effect of yield stress on dome wrinkling (low hardening rate).

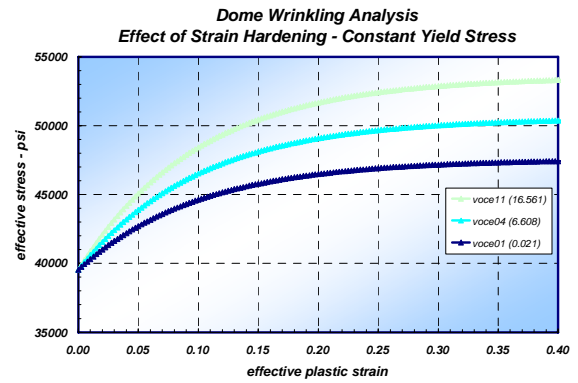


Figure 7. Effect of strain hardening on dome wrinkling – constant yield stress.

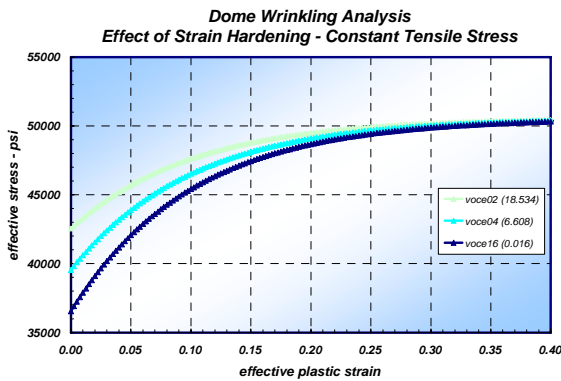


Figure 8. Effect of strain hardening on dome wrinkling – constant tensile stress.

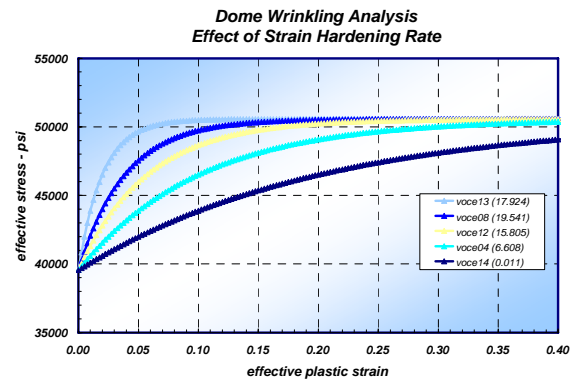


Figure 9. Effect of strain hardening rate on dome wrinkling.

### Effect of r-Value Directionalities on Wrinkling

FE simulations were also carried out using the Yld2000 [4] material model in order to assess the influence of planar anisotropy (different in-plane properties) on the wrinkling behavior. Stress and r-value directionalities are assumed to be isotropic except that the r-value at 45 degrees is taken as 2.0. Figures 10 and 11 show the progression of wrinkling and the comparison with the isotropic mode (Voce 08), respectively. For the isotropic model, seven wrinkles for a quarter section (28 wrinkles) were predicted. For planar anisotropy, however, 8 wrinkles were predicted for a quarter section (32 wrinkles). This was thought to be due to the effect which produces a non-uniform sheet thickness circumferentially and therefore, increases the susceptibility to wrinkling. Also, for planar anisotropy it has been found that the amplitude of wrinkling is reduced compared to the isotropic model especially along 45 degrees (high r-value region). This means that a lower in-plane compressive stress is needed to deform the material due to the influence of shear deformation from planar anisotropy, thus postponing wrinkling. The relative

magnitude of wrinkling may be determined based on the degree of planar shear deformation, which gives smaller amplitudes with an increased number of wrinkles.

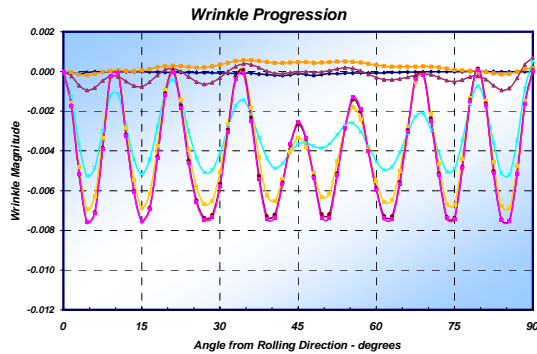


Figure 10. Progression of wrinkling

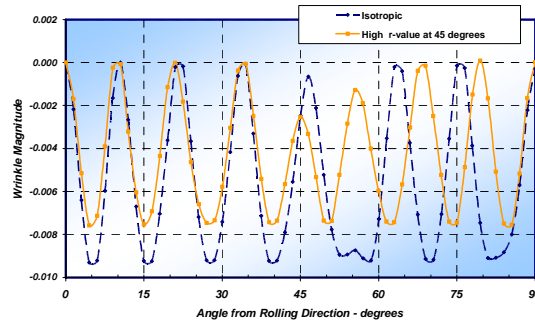


Figure 11. Comparison between isotropy and planar anisotropy.

## Summary

Wrinkling during the dome forming process was investigated in view of hardening and anisotropy. The results presented confirm the trends based on manufacturing experience. The study on material characteristics indicates that low plastic work minimizes dome profile wrinkling. However, there is a trade-off between wrinkling and structural performance. Factors that control or reduce wrinkling may also affect localized thinning or structural performance. An acceptable solution must balance formability and structural performance requirements. The effect of tooling friction should be investigated. Also, mesh refinement should be studied as a finer mesh will allow for a better approximation of the wrinkle shapes and will impact the wrinkle factor magnitude. However, the overall trends should remain the same.

## References

- [1] Chan, S.L.: *A non-linear numerical method for accurate determination of limit and bifurcation points*. Int. J. Num. Meth. Eng, 36: 2779-2790, 1993.
- [2] Cao, J., Boyce, M. C.: *Optimization of sheet metal forming processes by instability analysis*. Proceedings of NUMIFORM'95, A. A. Balkema, Rotterdam, 675-679, 1995.
- [3] Kim, J.B., Yoon, J.W., Yang, D.Y.: *Investigation into the wrinkling behavior of thin sheet on the cylindrical cup deep drawing process using bifurcation theory*. Int. J. for Numerical Methods in Eng, 56: 1673-1705, 2003.
- [4] Barlat, F., Brem, J.C., Yoon, J.W., Chung, K., Dick, R.E., Lege, D.J., Pourboghrat, F. Choi, S.H., Chu, E.: *Plane stress yield function for aluminum alloy sheets*. Int. J. Plasticity 19: 1297-1319, 2003.
- [5] Narayanasamy, R., Sowerby, R.: *Wrinkling of sheet metals when drawing through a conical die*. J. Mater. Process. Technol. 41: 275-290, 1994.

**Table 1.**  
**Dome Wrinkling Analysis – Voce Coefficient Data**

| <i>ID</i>                                                   | <i>Voce A<br/>(psi)</i> | <i>Voce B<br/>(psi)</i> | <i>Voce C</i> | <i>Yield<br/>Stress<br/>(psi)</i> | <i>Wrinkle<br/>Factor</i> | <i>Effective<br/>Plastic<br/>Strain</i> |
|-------------------------------------------------------------|-------------------------|-------------------------|---------------|-----------------------------------|---------------------------|-----------------------------------------|
| <b>DOX 2<sup>3</sup>Factorial Design</b>                    |                         |                         |               |                                   |                           |                                         |
| <i>voce01</i>                                               | 47572.                  | 8017.                   | 10.000        | 39555.                            | <b>0.0201</b>             | <b>0.443</b>                            |
| <i>voce02</i>                                               | 50572.                  | 8017.                   | 10.000        | 42555.                            | <b>18.534</b>             | <b>0.346</b>                            |
| <i>voce03</i>                                               | 47572.                  | 11017.                  | 10.000        | 36555.                            | <b>0.004</b>              | <b>0.457</b>                            |
| <i>voce04</i>                                               | 50572.                  | 11017.                  | 10.000        | 39555.                            | <b>6.608</b>              | <b>0.335</b>                            |
| <i>voce05</i>                                               | 47572.                  | 8017.                   | 25.887        | 39555.                            | <b>14.451</b>             | <b>0.312</b>                            |
| <i>voce06</i>                                               | 50572.                  | 8017.                   | 25.887        | 42555.                            | <b>17.401</b>             | <b>0.308</b>                            |
| <i>voce07</i>                                               | 47572.                  | 11017.                  | 25.887        | 36555.                            | <b>10.189</b>             | <b>0.317</b>                            |
| <i>voce08</i>                                               | 50572.                  | 11017.                  | 25.887        | 39555.                            | <b>19.541</b>             | <b>0.315</b>                            |
| <b>Effect of Yield Stress</b>                               |                         |                         |               |                                   |                           |                                         |
| <i>voce03</i>                                               | 47572.                  | 11017.                  | 10.000        | 36555.                            | <b>0.004</b>              | <b>0.457</b>                            |
| <i>voce04</i>                                               | 50572.                  | 11017.                  | 10.000        | 39555.                            | <b>6.608</b>              | <b>0.335</b>                            |
| <i>voce09</i>                                               | 53572.                  | 11017.                  | 10.000        | 42555.                            | <b>15.646</b>             | <b>0.296</b>                            |
| <b>Effect of Strain Hardening – Constant Yield Stress</b>   |                         |                         |               |                                   |                           |                                         |
| <i>voce01</i>                                               | 47572.                  | 8017.                   | 10.000        | 39555.                            | <b>0.0201</b>             | <b>0.443</b>                            |
| <i>voce04</i>                                               | 50572.                  | 11017.                  | 10.000        | 39555.                            | <b>6.608</b>              | <b>0.335</b>                            |
| <i>voce11</i>                                               | 53572.                  | 14017.                  | 10.000        | 39555.                            | <b>16.561</b>             | <b>0.322</b>                            |
| <b>Effect of Strain Hardening – Constant Tensile Stress</b> |                         |                         |               |                                   |                           |                                         |
| <i>voce02</i>                                               | 50572.                  | 8017.                   | 10.000        | 42555.                            | <b>18.534</b>             | <b>0.346</b>                            |
| <i>voce04</i>                                               | 50572.                  | 11017.                  | 10.000        | 39555.                            | <b>6.608</b>              | <b>0.335</b>                            |
| <i>voce16</i>                                               | 50572.                  | 14017.                  | 10.000        | 36555.                            | <b>0.016</b>              | <b>0.347</b>                            |
| <b>Effect of Strain Hardening Rate</b>                      |                         |                         |               |                                   |                           |                                         |
| <i>voce14</i>                                               | 50572.                  | 11017.                  | 5.000         | 39555.                            | <b>0.011</b>              | <b>0.489</b>                            |
| <i>voce04</i>                                               | 50572.                  | 11017.                  | 10.000        | 39555.                            | <b>6.608</b>              | <b>0.335</b>                            |
| <i>voce12</i>                                               | 50572.                  | 11017.                  | 17.500        | 39555.                            | <b>15.805</b>             | <b>0.320</b>                            |
| <i>voce08</i>                                               | 50572.                  | 11017.                  | 25.887        | 39555.                            | <b>19.541</b>             | <b>0.315</b>                            |
| <i>voce13</i>                                               | 50572.                  | 11017.                  | 50.000        | 39555.                            | <b>17.924</b>             | <b>0.303</b>                            |

